

# Atmospheric Impact of Volcano Eruptions

W. Engelke<sup>1</sup> \* A. Kuhn<sup>2</sup> † M. Flatken<sup>1</sup> F. Chen<sup>1</sup> H.-C. Hege<sup>2</sup> A. Gerndt<sup>1</sup> I. Hotz<sup>1</sup>

<sup>1</sup> Dept. Simulation and Software Technology - German Aerospace Center (DLR), <sup>2</sup> Zuse Institute Berlin (ZIB)

## 1 INTRODUCTION

The analysis of data that captures volcanic eruptions and their atmospheric aftermath plays an important role for domain experts to gain a deeper understanding of the volcanic eruption and their consequences for atmosphere, climate and air traffic. Thereby, one major challenge is to extract and combine the essential information, which is spread over various, mostly sparse data sources. This requires a careful integration of each data set with its strength and limitations. The sparse, but more reliable measurement data is mainly used to calibrate the more dense simulation data. This work combines a collection of visualization approaches into an exploitative framework. The goal is to support the domain experts to build a complete picture of the situation. But it is also important to understand the individual data sources, the wealth of their information and the quality of the simulation results. All presented methods are designed for direct interaction with the data from different perspectives rather than the sole generation of some final images.

The visualization methods have been developed on the basis of two different frameworks. The first is a modular and flexible software for fast development of visualization techniques developed at the German Aerospace Center (DLR). A major design principle of this tool is the ability to work interactively with the data. To achieve this the program uses massively the possibilities of modern programmable graphics hardware and multi core architectures. The easy to understand and easy to use node based graphical interface gives quick access to the four main resources for data loading, data operations, parameter adjustment, rendering and material handling. Editing shader code and CUDA kernels during run time makes fast development possible. The second framework we use is Amira, which is the development platform for most of the research projects at the department of visualization at Zuse Institute Berlin (ZIB).

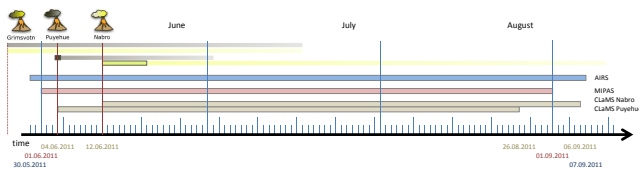


Figure 1: Overview over the temporal availability of the various data sets. Displayed are the three eruption events and the time span of the respective measurements or simulations. Whereas the Grimsvötn volcano ejected ash (gray bar) and sulfur (yellow bar) the Puyehue event was dominated by ash and the Nabro event by sulfur ejections.

\*e-mail: {Wito.Engelke,Markus.Flatken,Fang.Chen,Ingrid.Hotz}@dlr.de

†e-mail: {kuhn, hege}@zib.de

## TASK 1: INITIAL DATA INTEGRATION AND BROWSING

The first part of the visualization provides the foundation of the visualization framework. Its goal is to create a review of the situation.

The user can browse through the unbiased data from the various modalities in its original form. This comprises showing their coverage and sparseness. It allows to explore it from different perspectives (Fig. 2) and apply simple and intuitive filtering mechanisms. At this point we refrain from any interpolation.

**Context and reference frames** To display the data given over a four dimensional domain we offer different projections and reference frames. For the spatial dimensions we provide a spherical or a flat world map with latitude and longitude. The user can easily switch between the two representations and change, switch on and off background textures, locations of the volcanoes or airports.

The third dimension can be used either to display height or time information. The scales of this dimension can be easily adapted. The fourth, remaining dimension is optionally projected down (data summary, e.g. data for all times) or is used to slice the data (e.g. data for one fixed time or height value). Thereby the different data sources are displayed on demand. For the three dimensional representations it is possible to focus on specific times by moving semi-transparent temporal slices.

**Domain and attribute filters** To cope with cluttering, a basis functionality of the interface are filters that can be applied interactively to the domain or attribute space, either to select data (e.g. trajectories) or to clip their rendering. It is possible to connect an arbitrary number of filtering steps to dig out the interesting aspects of the data. The trajectories can be rendered as lines or tubes which are colored with respect to user-defined attributes (e.g. height, seeding time) or derived entities.

## TASK 2: LINKING MIPAS DETECTIONS TO ERUPTION EVENTS – PLUME EVOLUTION

In order to inspect the clouds associated to the individual volcano eruptions, we offer an implicit cloud rendering directly from the original data using the filter and rendering options of the basic framework. Alternatively, we also support two different ways to explicit generation of a density texture or geometry.

### 2.1 Implicit cloud rendering

This method uses a two-fold application of the filtering options described in Task 1. First, the filter is adjusted to the location of the volcanos and the time of the eruption. This selects all particles whose trajectories are traced back to the volcano at the time of eruption. Using a second filter limits the rendered trajectories to a short time span. Playing with the rendering parameters as trajectory diameter and the filter sizes gives a first estimate of the cloud. Moving this time-window shows how the cloud evolves over time. This perspective on the data only uses the CLaMS data set without taking the accuracy of the simulation into account which decreases with the integration (back tracing) times. Thus the resulting clouds are not very crisp. But due to the interactivity of this approach it helps to get a feeling for the distribution of the trajectories at the time of eruption and to find an appropriate window size (Fig. 3).

## 2.2 Explicit cloud texture generation

First we associate the MIPAS detections with the eruption events. This is done via the classification of the CLaMS trajectories, which is uniquely linked to the MIPAS detections. In a second step we use MIPAS data together with the associated CLaMS trajectories to generate a continuous ash or sulfur density field.

*CLaMS-trajectory proximity classification* – Here, we use the proximity of the trajectories to the respective volcanoes as an indicator for its origin. Later, we also consider a clustering approach as an alternative, see Sec. 2.3. To each volcano eruption one can assign a specific spatial and temporal window (Fig. 1). In reality an eruption can be considered spatially as a ‘point-event’, while the temporal specification is less precise and can be a time interval of a couple of days. From the implicit cloud rendering (Sec. 2.1) we know that only a portion of the trajectories passes these small windows. This is partially due to the limited accuracy of the particle simulation (long integration times, turbulence during the eruption). A further problem is that the back tracing of the particles stops at June first, which is ten days after the eruption of the Grimsvötn volcano and the position of the cloud at this time is not known. The size of the window is critical for the classification results. A first hint towards reasonable values can be derived from the implicit cloud rendering. To get a more quantitative impression of the impact of these parameters we generated a histogram with respect to the spatial window size (Fig. 4).

*Cloud texture generation* – The MIPAS classification alone is not sufficient to estimate the cloud evolution since it is too sparse. To fill the gaps between the individual detections we assign a ‘footprint’ to each detection to generate an ash or sulfur density data set, which is regularly sampled and stored in a 3D texture for each volcano (Fig. 5). This allows an efficient handling and rendering of the data. The three dimensions are associated to longitude, latitude, and time. The texture format (rgba) allows to store up to four parameters per pixel (density, minimum and maximum altitude). The fourth parameter is currently not used and is available for a user specified choice. The footprint for the interpolation is based on the CLaMS trajectories. For each trajectory passing a MIPAS detection an anisotropic footprint along the trajectory (for a given short temporal interval, weighted by the distance to the detection) is added (see Fig. 13). The short time window makes sure that only reliable (short term integration) parts of the trajectories are considered. The cloud altitude is store by its minimum and maximum values derived from the trajectories. Critical parameters for the texture generation are the temporal and spatial extend of the footprint. For small values the gaps will not be filled and for large values the shape of the cloud will be blurred. We further compare the results with AIRS data in Task 2.3.

## 2.3 Spatio-temporal trajectory clustering

In contrast to Sec 2.2, we generate the density texture without previous classification of CLaMS data resulting in one ash and one sulfur density texture. Based on this texture we generate isosurfaces in the space-time domain with a consecutive connected component analysis. We offer the option to discard small (volume below given threshold) components. Technically, we use a contour tree clustering approach that identifies hierarchical sets of isolevels within scalar fields and additionally allows for a persistence-based simplification of the underlying tree structure.

With this analysis, we are able to identify a group of larger clusters clearly associated to the three major events. In the meantime, we also spotted some clusters which are irrelevant to the given three volcanoes. While some of these clusters can be related to smaller scale eruptions (such as Lokon and Aetna volcanos), the origins of other clusters remain unknown.

## TASK 3: WHAT DOES AIRS ADD TO THE OVERALL PICTURE?

First we compare the AIRS images to our texture from the MIPAS/CLaMS interpolation (Fig. 6) introduced in Sec. 2.2. Thereby we only consider the accumulated density values without taking the height information into account due to the absence of altitude information in AIRS. We observe that the cloud pattern in our texture yields a plausible correspondence to the AIRS image at the time and regions where AIRS data is available. It is also observed that the AIRS data is finer at cloud boundaries showing sharper features. However, AIRS data captures the cloud structure (similar to streak lines or dye advection) in terms of ‘snapshots’. Therefore, such sharp features are only available at limited space-time domains. Furthermore, the sensitivity of AIRS images is much lower than that of the MIPAS data, meaning that the clouds dissolve much earlier than for the texture as shown in Figure 8. This may also be the reason for the larger extend of the texture clouds. Due to the sparseness of AIRS data in both spatial and temporal direction, direct interpolation of AIRS does not yield a feasible representation. Therefore, we provide a variety of possibilities to compare and to visually complete AIRS with other data sets (cf. Fig. 7 and 8), without explicitly merging them. One of our choices is to extract the topological skeleton of the clouds (i.e. maxima, saddle points, and ridge lines) which is less dependent on the data resolution and choice of interpolation parameters as shown in Fig. 11 and Fig. 12.

## TASK 4: HOW DID THE ERUPTION OF PUYEHUE-CORDÓN CAULLE AFFECT AIR TRAFFIC?

The AIRS data are in good agreement with the closing of the airports in Australia and New Zealand. Due to the absence of altitude information in AIRS data, we also inspected the ash cloud from MIPAS/CLaMS texture during the airport closings, allowing for further identification of dangerous flight zones (Fig. 9). Adding the common aircraft altitude (8 to 10 km) and the airports as context information into the 3D spatial ash cloud rendering gives us the impression that the airport closings have been justified. Our findings show that airports in Australia and New Zealand were disrupted during 10th and 13th of June due to volcanic ashes from Puyehue eruption (Fig. 9). Later this month, between the 15th and the 17th of June, air traffic above Argentinian airports are influenced. Around 22nd and 23rd, the ash cloud has already traveled around the globe once and re-entered Australian air spaces.

## TASK 5: HOW DID NABRO AEROSOL ENTER THE STRATOSPHERE?

By looking at the cluster of Nabro trajectories, we realize they are much higher than those from the other two volcanoes. To find out when and where the Nabro aerosol entered the stratosphere, first we collect all Nabro classified trajectories which intersect the stratosphere at some point. Then we draw a set of these trajectories into an altitude-time plot. This plot (Fig. 10) reveals the fact that vertical transport of the aerosol exists. By further linking the vertical transported lines to the spatial view, we observed that the majority of the lines which could potentially be responsible for vertical transportation (red lines in Fig. 10) are not passing the location of the volcano in lower altitudes. Only a few lines can be responsible for transportation of material from the volcano to the lower stratosphere (green lines in Fig. 10). These are integrated backwards for a long time in the simulation model. Therefore we tend to consider that the Nabro aerosol was directly injected into the stratosphere.

## ACKNOWLEDGEMENTS

We would like to thank Patrick Jöckel from Inst. of Atmospheric Physics - DLR for his support and explanations of the data domain. This work was partially funded by the German Federal Ministry of Education and Research under grant number 01LK1213A and by the European Union Framework Programme FP7 under grant agreement number 607177.

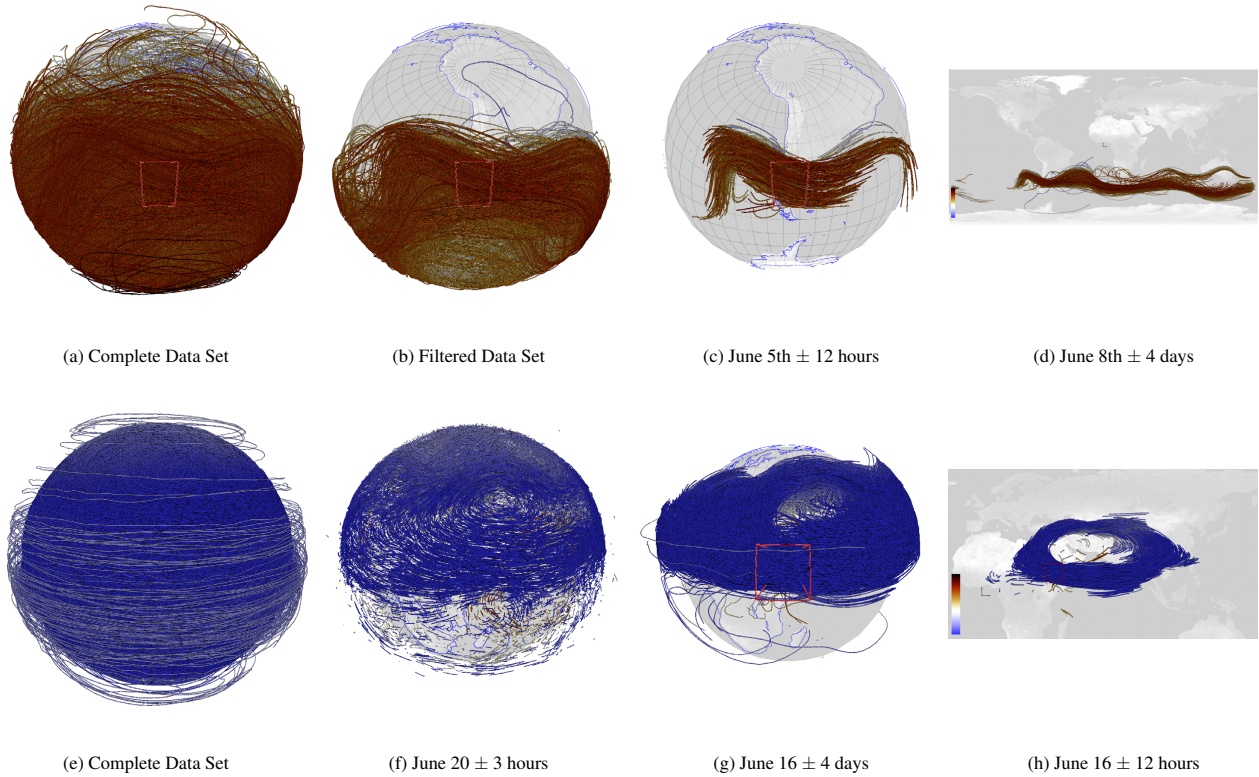


Figure 2: **CLaMS Data Sets.** *Top Row: Puyehue.* a) All trajectories, b) Space-time filtered trajectories on location of volcano  $\pm 5^\circ$  in longitude and latitude, c) Space-time filtered trajectories on location of volcano  $\pm 5^\circ$  in longitude and latitude and from May 30th to June 6th in time, d) Space-time filtered trajectories on location of volcano  $\pm 5^\circ$  in longitude and latitude and from May 30th to June 6th in time. Color is mapped to altitude ranging from 0 km to 18 km. All images use the same colorscale. *Bottom Row: Nabro.* e) All trajectories, f) all trajectories on June 20th  $\pm$  3 hours, g) Space-time filtered trajectories on location of volcano  $\pm 5^\circ$  in longitude and latitude and from June 12th to June 20th in time, h) ROI: space-time filtered trajectories on location of volcano  $\pm 5^\circ$  in longitude and latitude and from June 12th to June 20th in time. Color is mapped to temperature ranging from  $184^\circ K$  to  $317^\circ K$ . All images use the same colorscale.

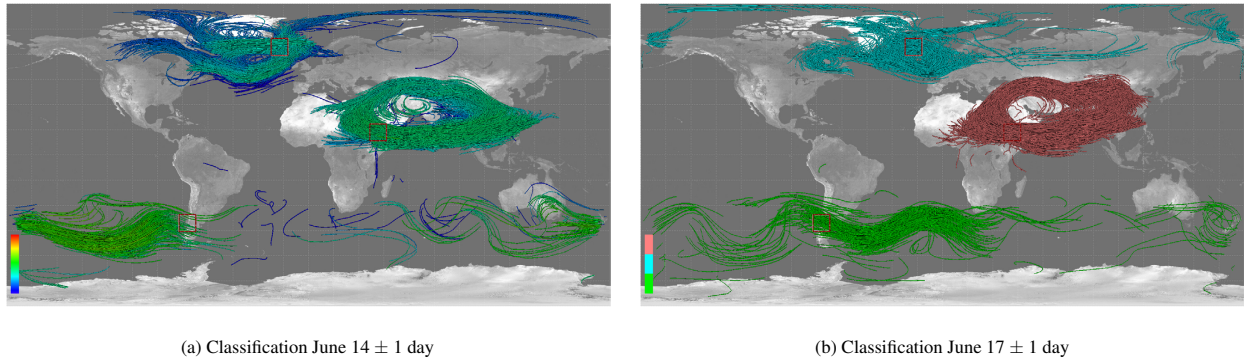


Figure 3: **CLaMS Data:** Classification based on distance to volcano. Space-time filters are applied for CLaMS data with the location of the volcanoes (Grimsvötn, Nabro and Puyehue)  $\pm 5^\circ$  in longitude and latitude, from June 1st to June 20th for the Grimsvötn, from June 12th to June 20th for the Nabro and from May 30th to June 7th in time for the Puyehue volcano. Images are showing the trajectories for two different days. Line color in a) is based on altitude ranging from 0 to 32,4 km, in b) the line color encodes the cluster ID. The red cluster contains 3705, the cyan cluster contains 1144 and the green cluster 429 trajectories. The shown images also demonstrate the flexibility of the used software. The user can interactively change mapped data properties, shown time step and time interval as well as filter properties such as filter region and filtered data properties.

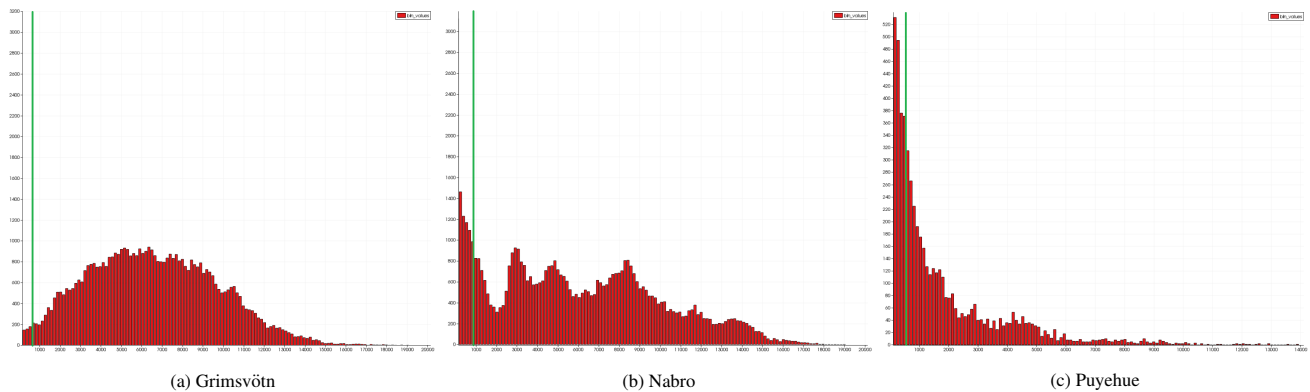


Figure 4: **Histogram:** Number of pathlines dependent on the distances to the respective volcanoes with a bin count of 128. a) Grimsvötn. The histogram does not show a clear peak. We decided to use a distance of 500 km. b) Nabro: The histogram shows a peak within a radius of 850km. There are also other local maximums where the trajectories could belong to other  $SO_2$  sources. c) Puyehue: The histogram shows a clear peak within a radius of 250km. The chosen radii are marked in the histograms.

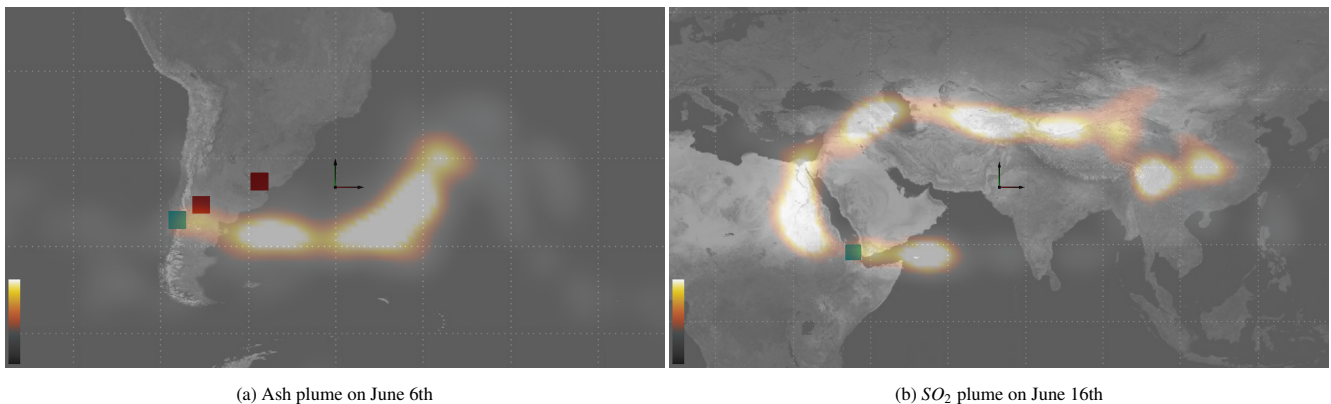


Figure 5: **Ash and  $SO_2$  plume:** Snapshot of the temporal evolution of the a) ash and b)  $SO_2$  plume. Marked in red are two airports in south America. Marked in cyan the locations of volcanoes

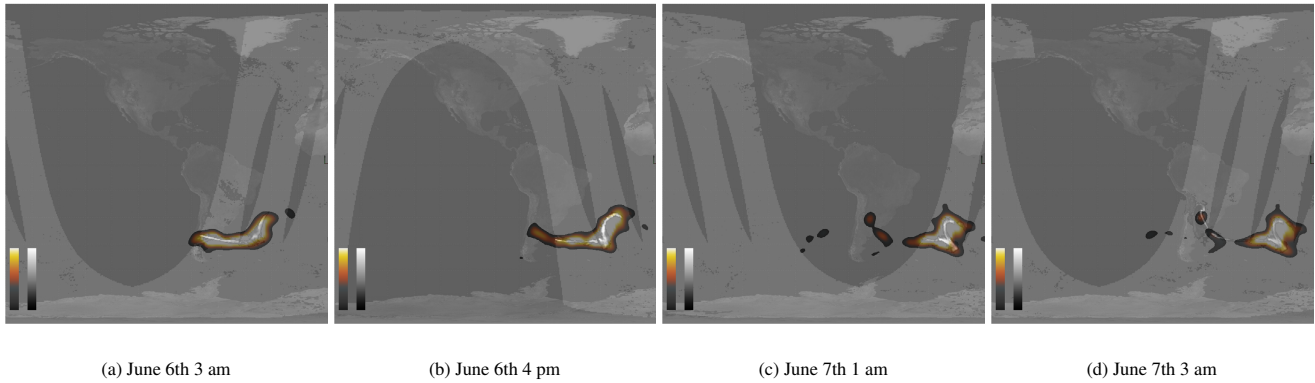


Figure 6: **Ash and SO<sub>2</sub> plume:** Snapshots of the temporal evolution of our combined MIPAS and CLaMS data for the tracking of the Puyehue ash plume against the AIRS data set. Our combined data has clear advantages over AIRS in temporal resolution whilst the AIRS data is able to deliver more spatial accuracy in terms of plumes shape and ash concentration.

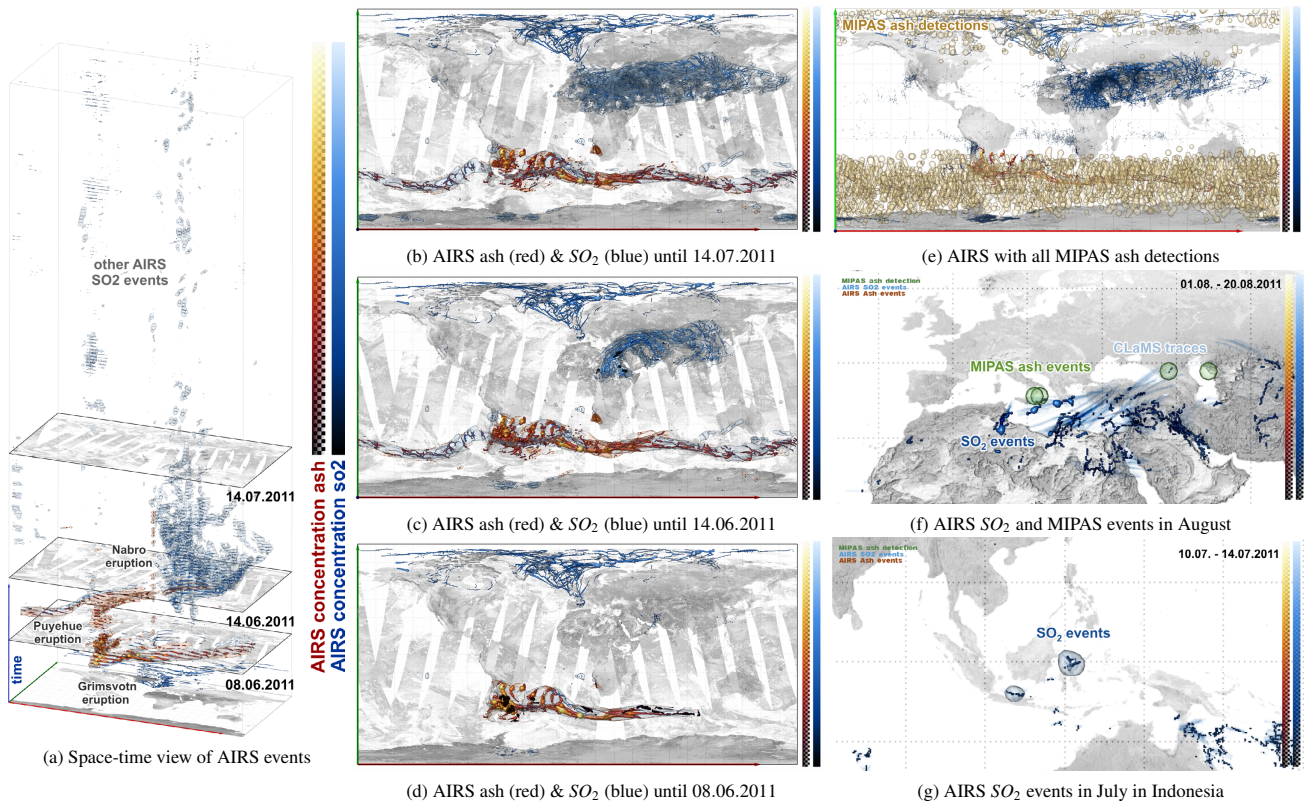
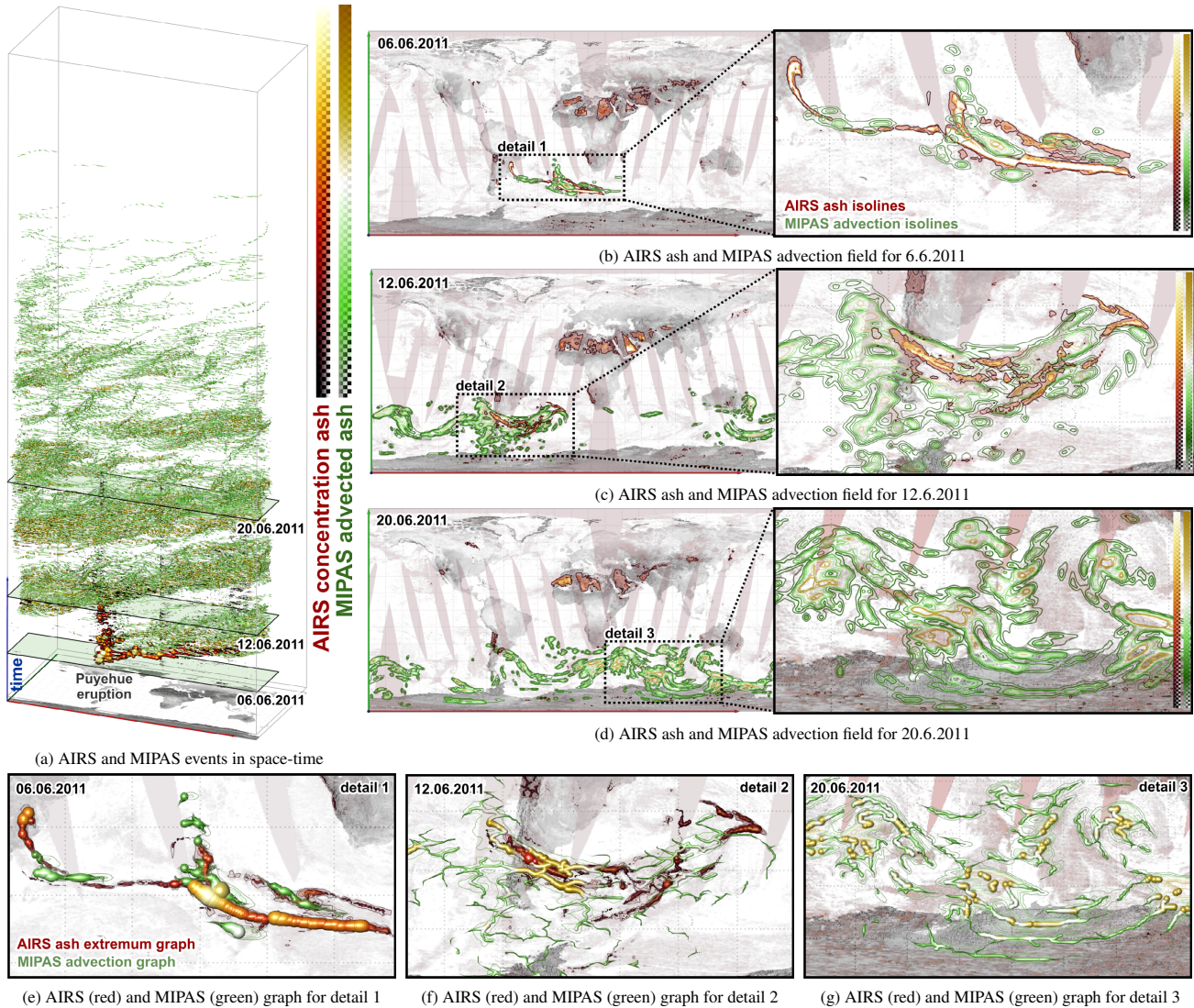


Figure 7: **AIRS, CLaMS, MIPAS:** AIRS data can be used to analyze SO<sub>2</sub> and ash concentration during the eruption events in space and time in Fig. a). The extraction of extremal points and ridge structures (colored and sized by the respective field value) emphasize locally strong production events in both quantities in Fig. b) and d). The high spatial resolution of AIRS data further captures additional small scale SO<sub>2</sub> production events e.g., in Europe at the beginning of August 2011 and an eruption of the Lokon-Empung (Indonesia) in July 2011.



**Figure 8: Combining AIRS, MIPAS and CLaMS:** Comparison of the AIRS ash data and the advected MIPAS ash field for the Puyehue-Cordon Caulle eruption. a) shows all extremum graphs combined in space-time; b) to d) show detailed isolines for both fields. e) to g) show the extremum graphs extracted for both modalities. The detail views reveal the strengths and weaknesses of both information sources: AIRS captures even fine spatial cloud structures, but suffers a limited detection accuracy (i.e., the ash cloud cannot be traced anymore after mid of June). MIPAS advection fields are more sensitive, but do not convey information about the actual strength of the detection and sometimes miss samples across thin cloud structures; advection by CLaMS trajectories helps to reconstruct parts of the missing information.

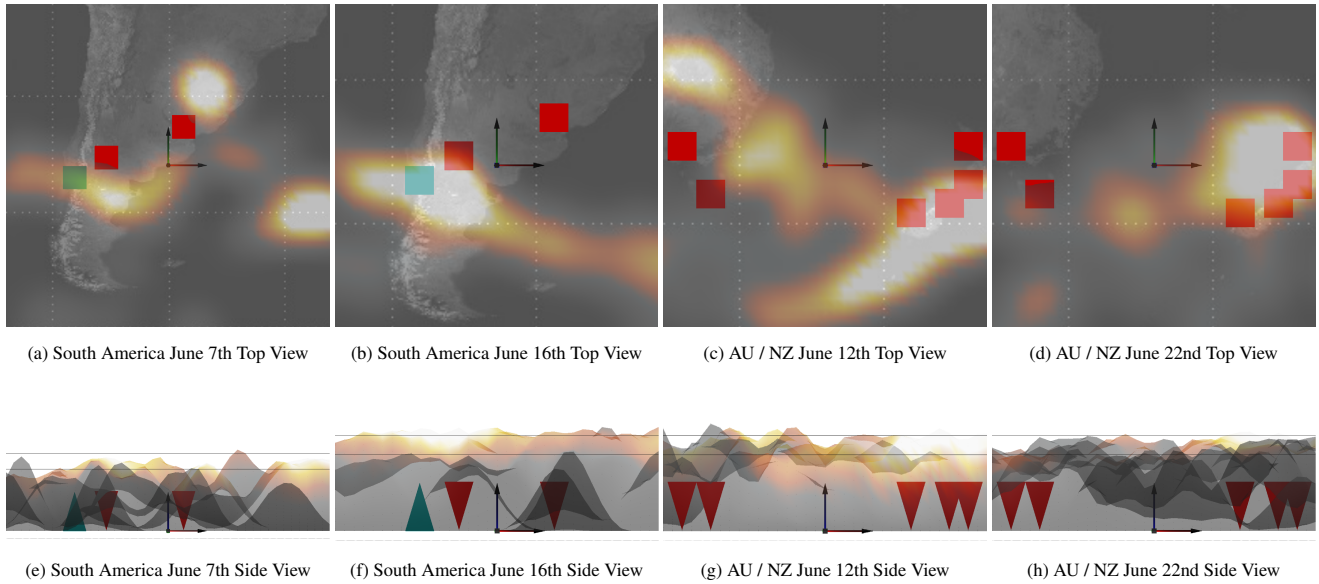


Figure 9: **Air traffic disruptions:** Closed Airports marked in cyan and movement of ash cloud are related. Closed Airports can be found in Argentina, Australia and New Zealand. Volcanoes are marked in cyan and airports in red. The side view shows two lines in 8 and 10 km height. This is the usually used cruising altitude for short and long range flights. Additionally the shown surface for the ash clouds is visualized with the local maximal height.

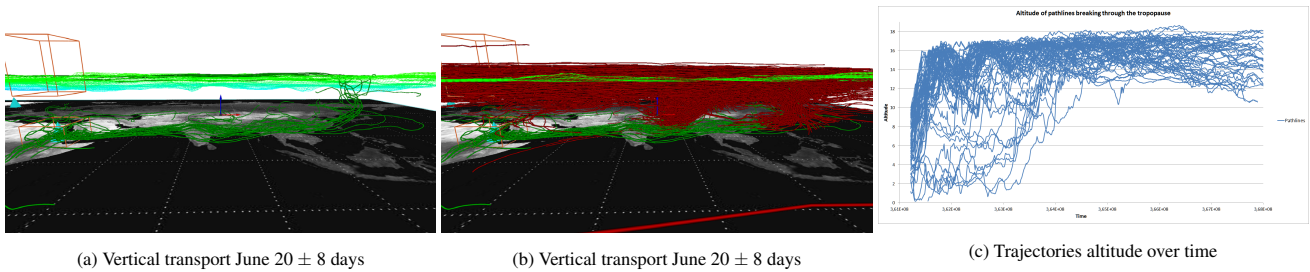


Figure 10: **CLaMS Nabro Data:** Vertical transport behavior can be seen in these two images. The line's color encodes the two clusters. a) The green cluster contains trajectories which can be responsible for vertical transport of material (e.g. ash) in the lower stratosphere, since they fulfill two criteria: first, they pass the geographic region near the volcano during the eruption period and they reach the lower stratosphere (e.g. they have a theta value  $> 380K$ ). The second cluster (red) transports material from the lower and upper troposphere to the lower stratosphere above India. But we were not able to find trajectories which reach the location of the volcano during its eruption period.

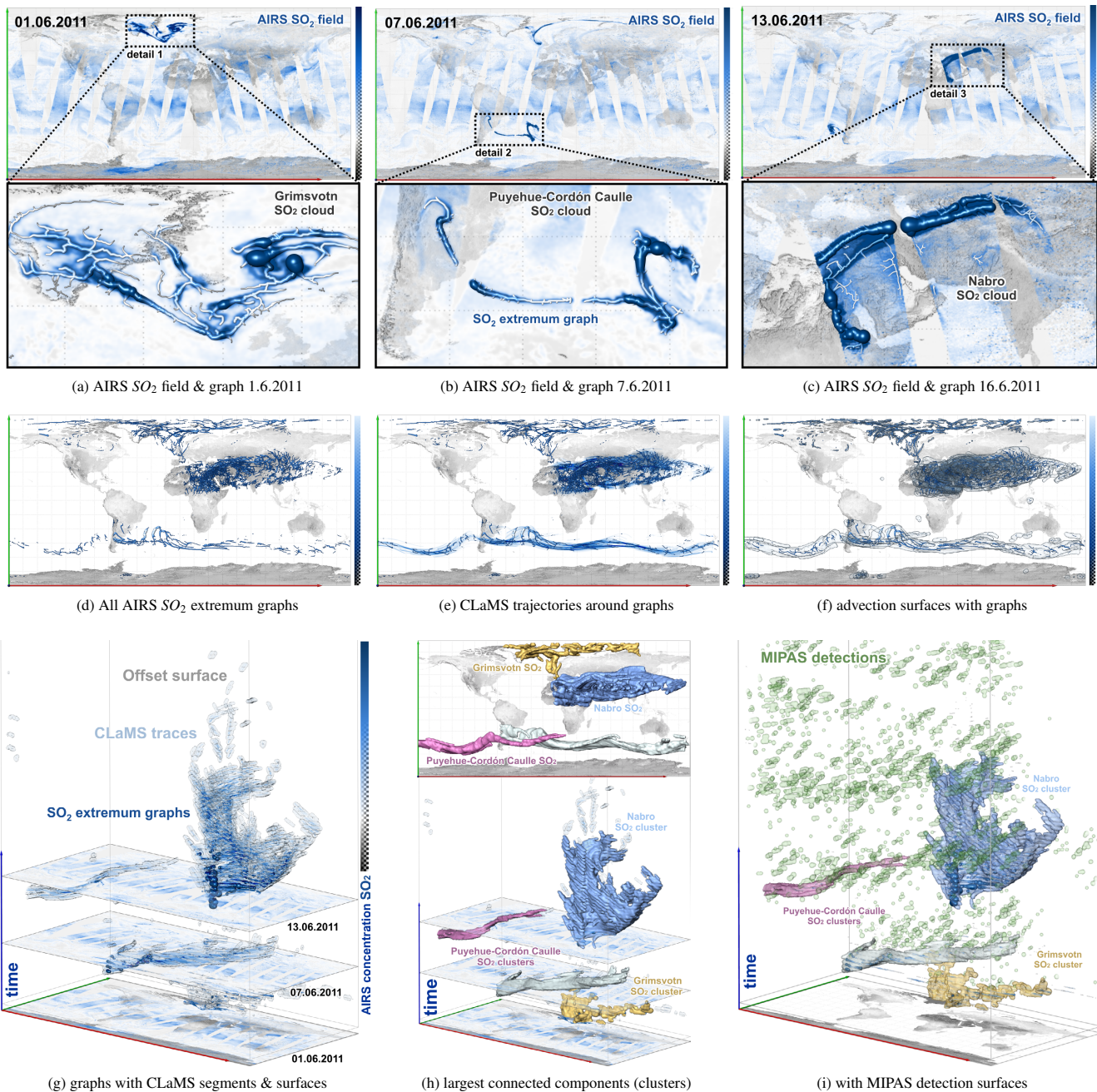


Figure 11: **Combining AIRS and CLaMS data:** Combining AIRS and CLaMS data allows to describe the spatio-temporal structure of occurring  $SO_2$  events and characterize the evolution of the  $SO_2$  plumes in each case: The Puyehue-Cordon Caulle  $SO_2$  cloud moves rapidly eastwards, following the major jet streams on the southern hemisphere. In contrast, the Nabro event remains 'trapped' in a larger vortex structure and is distributed across central Asia while Grimsvötn  $SO_2$  cloud circulates towards the north pole. The space-time view of multiple modalities in g) conveys location and time of strongest value concentrations and their distribution during the plume development. A connected component analysis allows to derive cluster volumes (filtered by volumes larger than 10.000 cells) that can be used to classify further information sources and events (e.g., CLaMS trajectories or MIPAS samples).

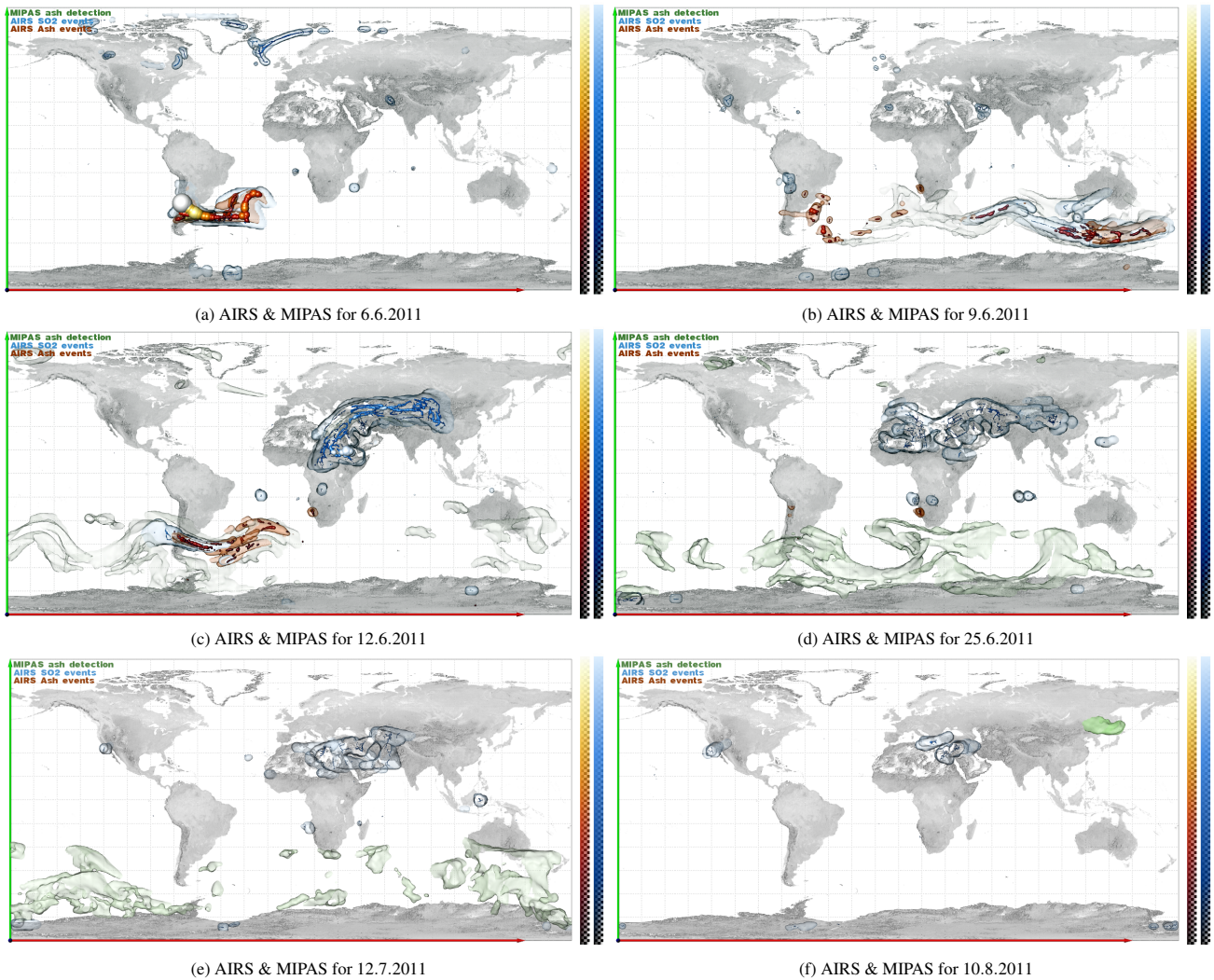


Figure 12: **Integrated Visualization:** This image shows six snapshots of an integrated visualization of AIRS SO<sub>2</sub> (blue) and AIRS ash (red) with its corresponding graphs (scaled and colored by AIRS value) and MIPAS advection surfaces (green transparent surfaces). Each images captures the situation of one day and highlights the different characteristics of the Puyehue-Cordon Caulle and the Nabro eruptions, especially with respect to ash production. The full animation is covered in the accompanying video.

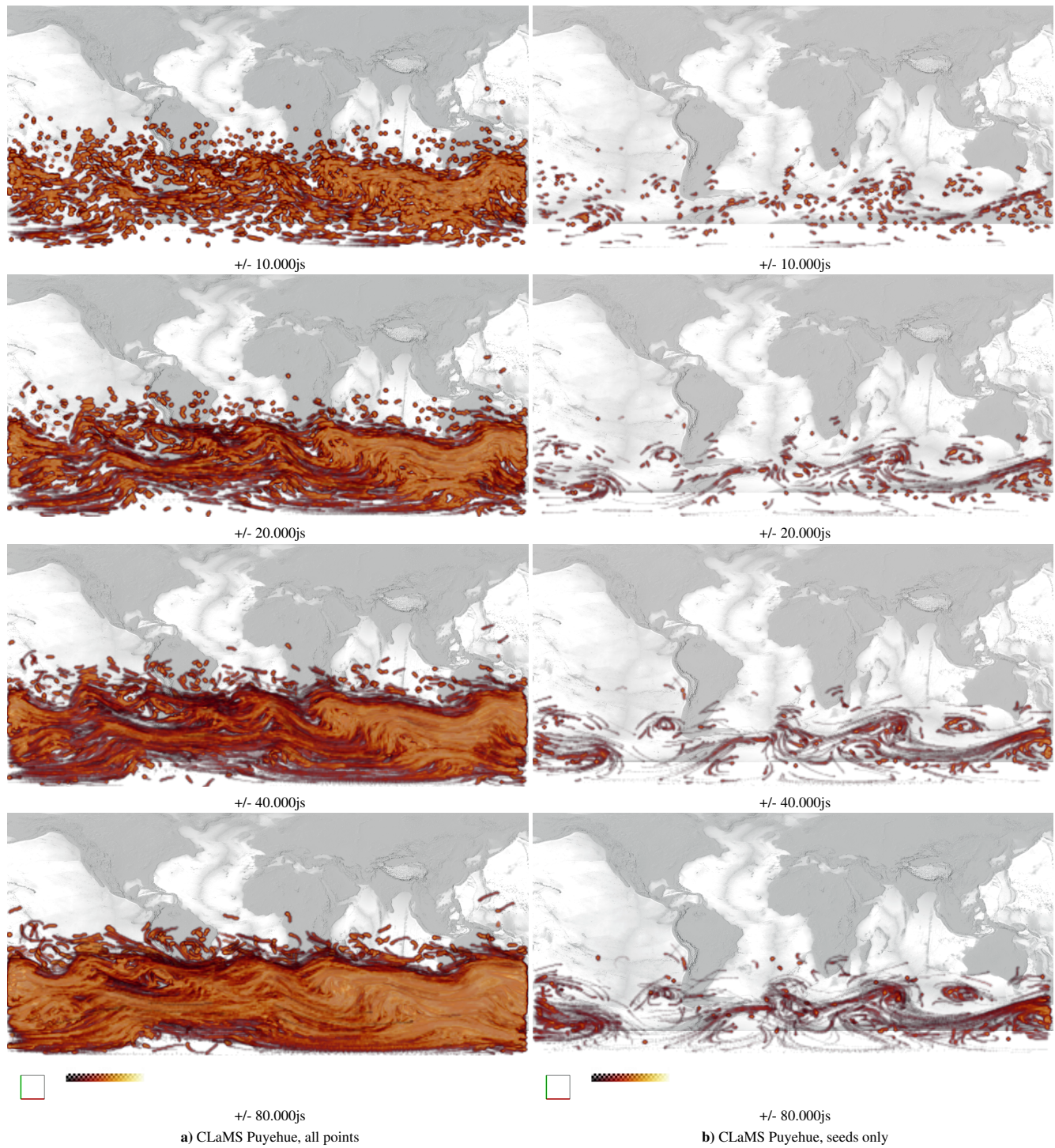


Figure 13: **CLaMS Advection Procedure:** Showing the effect of an increased temporal filter range on the CLaMS-Puyehue line set. The color indicates the spatio-temporal distance to the next sampling point in a 360x180x200 grid. The seeding points have been spread spatially using a 3x3x3 Gauss filter ( $\sigma = 0.4$ ).